Incorporation of proteins into complex coacervates

Whitney C. Blocher McTigue[a], **Sarah L. Perry**[a,b,*]
[a]Department of Chemical Engineering, University of Massachusetts Amherst, Amherst, MA, United States
[b]Institute for Applied Life Sciences, University of Massachusetts Amherst, Amherst, MA, United States
*Corresponding author: e-mail address: perrys@engin.umass.edu

Contents

Abstract

Complex coacervates have found a renewed interest in the past few decades in various fields such as food and personal care products, membraneless cellular compartments, the origin of life, and, most notably, as a mode of transport and stabilization of drugs. Here, we describe general methods for characterizing the phase behavior of complex coacervates and quantifying the incorporation of proteins into these phase separated materials.

Methods in Enzymology
ISSN 0076-6879
https://doi.org/10.1016/bs.mie.2020.06.006

1. Introduction

The encapsulation of proteins and other biomacromolecules is an area of tremendous activity, as such materials are finding increasing utility in applications such as drug delivery, environmental remediation, personal care products and biocatalysis. Proteins are generally very sensitive to their environment, and typical methods used for encapsulation can decrease or even destroy the activity of these molecules. Complex coacervation is a method that can be used to encapsulate proteins without using harsh conditions that may denature the protein cargo. This method of sequestration is a viable platform for a variety of different areas such as food science (Schmitt & Turgeon, 2011; Yeo, Bellas, Firestone, Langer, & Kohane, 2005), personal care products (Carvalho, Estevinho, & Santos, 2016; Martins, Barreiro, Coelho, & Rodrigues, 2014), and medicine (Kuo et al., 2014), because of the ability to generate biocompatible formulations and drive high levels of encapsulation without the need for organic solvents (Black et al., 2014; Kishimura, Koide, Osada, Yamasaki, & Kataoka, 2007; Vehlow et al., 2016; Water et al., 2014).

1.1 Complex coacervation and protein incorporation

Complexation occurs when oppositely-charged polyelectrolytes interact under favorable conditions such that the electrostatic attraction and entropic gains can drive phase separation. Coacervation is a purely aqueous strategy that can also be leveraged for the triggerable release protein cargo (Lim, Ping, & Miserez, 2018; Lindhoud, de Vries, Schweins, Cohen Stuart, & Norde, 2009); Lindhoud, Voorhaar, et al., 2009. These materials are versatile and have been shown usable for various delivery techniques such as an injectable protein carrier (Johnson & Wang, 2013, 2014; Nishida, Tamura, & Yui, 2018) and for oral delivery (Bourganis, Karamanidou, Kammona, & Kiparissides, 2017; Chapeau et al., 2017). This method will focus on using complex coacervation as an aqueous protein encapsulation technique, and experimental strategies related to characterizing the concentration of protein present in such formulations.

1.2 Complex coacervate phase behavior

There are many variables that alter the ability of polyelectrolytes to undergo complex coacervation, including the salt concentration, pH, charge density

and chemistry of the polymers, etc. Here, we will describe an experimental strategy for characterizing aspects of the phase behavior of complex coacervates, without consideration for other formulation-relevant questions such as the size and temporal stability of a dispersion of coacervate droplets etc. One consequence of this experimental focus is the use of concentration on an ionizable monomer basis, rather than units of mass of polymer per volume that are more typical when considering polymeric materials. Furthermore, this discussion assumes that the coacervate materials in question are able to fully equilibrate (i.e., form liquid droplets, rather than kinetically-trapped gels or solid complexes).

Complex coacervation involves the interaction of oppositely-charged polyelectrolytes. Thus, while physical and chemical aspects of the polymer such as length, charge density and/or degree of ionization, as well as hydrophobicity can modulate the phase behavior, we can typically rely on general intuition regarding electrostatic effects and charge neutrality. For complex coacervation, the ability to phase separate will be maximized when an equal number of oppositely-charged groups are present. While this condition may be straightforward to predict with some simple polymer systems, factors such as pH-dependent degree of ionization can play a role. These effects are highlighted in Fig. 1A and B, which show schematic depictions of a two-dimensional phase diagram as a function of the concentration of polycation and polyanion, with the concentration of salt present in the system defining the contours. The height (i.e., salt stability) of the two-phase region is maximized along the line of equimolar charge (black line). For systems where all of the potentially ionizable monomers are charged, this results in a symmetric phase diagram (Fig. 1A). However, if the pH of the solution has been changed such that only half of the ionizable groups on one of the polymers are charged (e.g., the apparent pKa of the polycation), then the phase diagram becomes asymmetric, as in Fig. 1B.

These same trends can be observed through a "stoichiometry" experiment, which typically uses turbidity to determine the polymer ratio that gives maximum coacervate yield (Chollakup, Beck, Dirnberger, Tirrell, & Eisenbach, 2013; Chollakup, Smitthipong, Eisenbach, & Tirrell, 2010; Cummings & Obermeyer, 2018; Obermeyer, Mills, Dong, Flores, & Olsen, 2016; Perry, Li, Priftis, Leon, & Tirrell, 2014; Priftis, Megley, Laugel, & Tirrell, 2013; Priftis & Tirrell, 2012). A stoichiometry experiment varies the relative amount of polycation to polyanion while keeping the total polymer concentration constant (corresponding to the gray lines in Fig. 1A and B). For systems where the polycation and polyanion can be considered as

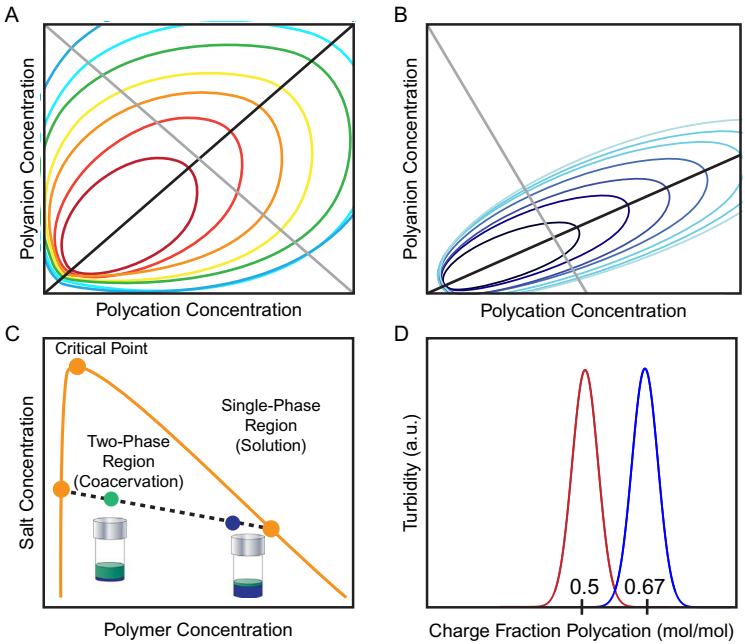

Fig. 1 A schematic contour plot of the three-dimensional phase envelope for complex coacervation as a function of relative polycation concentration, polyanion concentration, and salt concentration (shown as contours) for (A) a system where the relative degree of ionization of the polycation and polyanion is the same, and (B) a system where the relative degree of ionization for the polycation is half that of the polyanion. The black line in both plots indicates the salt-polymer phase behavior for a mixture of equal numbers of ionized cationic and anionic species, shown as the binodal curve in (C). The gray line traces out the effect of changing the charge stoichiometry of the system. (C) A schematic illustration of a typical salt vs. polymer concentration phase diagram defined by the black lines in (A and B). Coacervation occurs in the two-phase region beneath the binodal curve. A sample prepared within this two-phase region will phase separate into a polymer-dense coacervate phase and a polymer-poor supernatant phase, connected by a tie-line. While identical coacervate and supernatant phases will be formed from any sample prepared along such a tie-line, the relative position on the line dictates the fraction of the resulting sample that will be coacervate vs. supernatant, as per the lever rule. A sample prepared at relatively high polymer concentration (blue dot) will produce a much larger volume of coacervate than one prepared at lower polymer concentrations (green). The relative volumes of coacervate (blue) and supernatant (green) are indicated in the depicted vials. (D) Schematic depiction of the results of a stoichiometry experiment, which tests the effect of changing the relative amounts of polycation and polyanion at constant total polymer concentration and constant solution conditions. The turbidity signal maps out conditions where phase separation occurs. For the system where the degree of ionization of the polymeric species is the same, a maximum in turbidity is observed at a charge fraction of 0.5 (red, corresponding to the gray line in (A)). This result shifts to a cationic charge fraction of 0.67 if the degree of ionization of the polycation is half that of the polyanion (blue, corresponding to the gray line in (B)).

fully ionized (or have equal levels of ionization), the peak in the turbidity would be expected at a mole fraction of 0.5 with respect to one of the polymer species, or a 1:1 equimolar ratio (Fig. 1D, red curve). However, if one of the polymer species is only half charged, this will result in a shift in the observed signal. For instance, in the example shown in Fig. 1B where only half of the monomers on the polycation are ionized, a turbidity peak would be observed at a charge fraction of 0.67, corresponding to the condition where two cationic monomers are needed for every one anionic monomer, or a 1:2 ratio (Fig. 1D, blue curve). This condition of charge neutrality identifies the point where the maximum number of polymer chains will be incorporated into the coacervate phase; complexation will still occur at off stoichiometric conditions, but with a decreased level of coacervation. From a theoretical perspective, the composition of the bulk coacervate phase should be the same, with the difference being purely one of yield. However, experimentally, the preparation of off-stoichiometry dispersions of coacervate droplets can result in the recruitment of excess polymer to the surface of the droplet, imparting colloidal stability (Perry et al., 2014; Priftis & Tirrell, 2012).

For a given ratio of polycation-to-polyanion, the phase diagram for coacervation is then shown as a one-dimensional binodal curve, typically as a function of salt and total polymer concentration (Fig. 1C). This binodal curve represents the slice through the larger two-dimensional phase space at constant polymer composition (i.e., the black line). Samples prepared at a composition within this two-phase region will phase separate into two liquid phases, the polymer-rich coacervate phase and the polymer-poor supernatant phase. The composition of the resulting coacervate and supernatant phases is defined by the tie-line that connects these two points. One interesting (and potentially unintuitive) result of this phase behavior is that increasing the amount of polymer present in the initial sample mixture will not result in a commensurate increase in the polymer concentration in the resulting coacervate phase. Instead, samples prepared at different points along the tie-line will result in samples with different quantities of the same coacervate phase, as defined by the lever rule. Samples prepared at higher polymer concentrations will result in a larger coacervate volume, and vice versa.

There are numerous strategies for weakening or completely overcoming the interactions that cause complex coacervation. For example, changes in the solution pH or the addition of an excess of one of the polymers can shift the solution conditions outside of the two-phase window (Comert & Dubin, 2017; Kaibara, Okazaki, Bohidar, & Dubin, 2000). As suggested

by Fig. 1A–C, ionic strength is also an important variable for controlling coacervation (Lindhoud, de Vries, et al., 2009; Lindhoud, Voorhaar, et al., 2009; Perry et al., 2014). The addition of salt can facilitate screening of the electrostatic interactions and reduces the entropic gains associated with complexation (Perry et al., 2014; Yan et al., 2013). However, it is important to define the conditions for which this salt dissolution is being defined. As shown in Fig. 1C, the *critical point* is the highest salt concentration for which phase separation can be observed. However, most experiments do not operate near the critical condition and are therefore interested in determining the concentration of salt above which phase separation is no longer observed for a given sample condition. This salt concentration is typically referred to as the salt resistance (Li et al., 2018; Madinya, Chang, Perry, & Sing, 2020), and is dependent upon the choice of polymers, the coacervate composition, and the identity of the salt used. As was discussed regarding the effects of polymer concentration on coacervate composition, the salt resistance for any sample prepared along a given tie-line will be the same. However because tie-lines for coacervation tend to be non-horizontal (i.e., there is preferential partitioning of salt out of the coacervate phase), it is possible to change the salt resistance by changing polymer concentration, although this usually requires a significant change so as to move off of one tie-line and onto another (Chang et al., 2017). In the context of encapsulation studies, the salt resistance is an important parameter because it determines the concentration of salt required to dismantle the coacervate.

This introduction is intended to provide a foundational understanding of coacervate phase behavior to facilitate the use of coacervation for protein encapsulation. Thus far, our discussion has focused on complex coacervates formed from two species, a polycation and a polyanion. While the addition of protein does not alter these design rules, the chemical complexity of proteins can make interpretation of experimental data more challenging. For instance, most proteins carry a mixture of positive and negative charges. While electrostatic intuition would dictate that we consider only the net charge of a protein, there are examples where clustering of charges has allowed for complex coacervation to occur "on the wrong side of the isoelectric point," such that it would *appear* that complexation is occurring between two species of the same charge (Comert, Malanowski, Azarikia, & Dubin, 2016; Cooper, Dubin, Kayitmazer, & Turksen, 2005; Xu, Liu, Faisal, Si, & Guo, 2017; Xu, Mazzawi, Chen, Sun, & Dubin, 2011). It is also common to explore coacervation between a protein and two

oppositely-charged polymers, particularly for cases where the protein of interest is only weakly charged (Blocher McTigue & Perry, 2019; Lindhoud & Claessens, 2016; Lindhoud, de Vries, et al., 2009; Lindhoud, Voorhaar, et al., 2009). In these cases it is necessary to consider the net charge of all three species, and to carefully balance the ionic strength of the system, as changes in the salt concentration will disfavor the incorporation of the more weakly charged protein in favor of stronger electrostatic interactions between the two more strongly charged polymers.

In the following sections we will discuss experimental strategies to characterize the coacervation phase behavior of a system of two oppositely-charged polymers containing a protein cargo, as well as the incorporation of protein into the coacervate phase. These methods are intended to be general, and can be adapted to fit specific situations, such as the complexation of a protein with only a single, oppositely-charged polymer.

2. Materials, equipment, and reagents

The materials required for these experiments include two oppositely-charged polyelectrolytes, a protein of interest, salt, buffer (if desired), and acid/base for pH adjustments. We recommend that all solutions of polymer, protein, buffer (if desired) and salt be adjusted to the same pH. Coomassie brilliant blue G-250 dye can be purchased alone or as part of a Bradford assay kit.

Samples will be prepared via pipetting in microcentrifuge tubes and transferred into well plates (96- or 384-well plates are common). We recommend the use of a vortex mixer during sample preparation, an optical microscope for sample visualization, and a plate reader with UV/vis spectrophotometry capabilities. It is also possible to perform samples in cuvettes using a UV/vis spectrophotometer. Turbidity measurements are typically performed at a wavelength of light in the middle of the visible spectrum, and away from the absorbance peak of any of the materials (~562 nm is common). For quantifying the concentration of protein present, the Coomassie dye used in the Bradford assay is analyzed at a wavelength of 595 nm, and the experiment can be performed in a well plate, cuvette, or other small volume UV/vis setup (e.g., NanoDrop). The use of absorbance at 280 nm requires the use of either UV-compatible cuvettes or a NanoDrop-type setup.

3. Safety considerations

These techniques are safe to perform in a standard laboratory setting with the use of appropriate personal protection equipment such as safety glasses, lab coats, and gloves. It is recommended that experiments involving Coomassie dye be performed inside a chemical fume hood. For specific materials, refer to the safety data sheets.

To keep solutions sterile and dust free, keep the lids on all reagents, removing the lid only when pipetting, placing the cap back each time, though the lid may remain loose. Similarly, we recommend keeping all microcentrifuge tubes closed except when adding solution or transferring samples. The presence of dust can alter turbidity results. Care should also be taken to avoid cross-contamination of samples from pipette tips.

4. Protocols

4.1 Characterizing coacervate phase behavior

While the ultimate goal of an experiment might be the encapsulation of a target protein, we recommend first characterizing the phase behavior of your coacervate system in terms of charge stoichiometry and salt resistance. These information will help in the planning of experiments related to protein encapsulation and will facilitate the interpretation of the resulting protein encapsulation data. These experiments are typically performed at relatively low concentrations of protein and polymer to limit reagent requirements. All experiments can be scaled up in terms of volumes and/or concentrations, though it is important to ensure that all samples are fully mixed and equilibrated.

4.2 Polymer-polymer stoichiometry experiments

Stoichiometry experiments examine coacervate formation as a function of the ratio of polycation to polyanion at constant polymer concentration. Thus, while polymer stock solutions can be prepared at any concentration, we recommend the use of ionizable monomer concentration on a molar basis. The use of monomer concentration circumvents issues with polymer polydispersity, and allows for the easy analysis of results in terms of the stoichiometry of electrostatic interactions. A stock solution concentration of 10 mM monomer is generally sufficient for turbidity experiments.

A typical stoichiometry experiment will span the range of possible charge fractions, which we will express in terms of the mole fraction of ionizable monomers of the polycation present in our sample, to observe both a peak in the data, and clear baselines. The data in Figs. 3 and 4 and the experimental recipes listed in Tables 1 and 2 span the range of 0.1–0.9. These data points can be equally spaced for initial experiments. However, once the location of the turbidity peak is known (or if its location is estimated based on the charge state of the polymers), it is useful to sample the concentration space around the peak more closely. Additionally, it is important to ensure that the final polymer concentration in the prepared samples results in a sufficiently high level of turbidity. This signal should be distinguishable

Table 1 Sample preparation for complexation between poly(L-lysine) (K_{50}) and poly(D,L-glutamate) (E_{50}), degree of polymerization $N = 50$, pH 7.0.

	Charge fraction $K_{50}(+)$	Volume 10 mM $E_{50}(-)$ (μL)	Volume 10 mM $K_{50}(+)$ (μL)	Volume water added (μL)
1	0.100	10.8	1.2	108.0
2	0.200	9.6	2.4	108.0
3	0.300	8.4	3.6	108.0
4	0.400	7.2	4.8	108.0
5	0.425	6.9	5.1	108.0
6	0.450	6.6	5.4	108.0
7	0.475	6.3	5.7	108.0
8	0.500	6.0	6.0	108.0
9	0.525	5.7	6.3	108.0
10	0.550	5.4	6.6	108.0
11	0.575	5.1	6.9	108.0
12	0.600	4.8	7.2	108.0
13	0.700	3.6	8.4	108.0
14	0.800	2.4	9.6	108.0
15	0.900	1.2	10.8	108.0
Blank	–	0.0	0.0	120.0

Components were added from right to left as outlined in the protocol. The final monomer concentration is 1 mM.

Table 2 Sample preparation for a salt curve for between poly(L-lysine) (K_{50}) and poly(D,L-glutamate) (E_{50}), degree of polymerization $N = 50$, in 10 mM HEPES buffer pH 7.0.

	Charge fraction $K_{50}(+)$	Volume 10 mM $E_{50}(-)$ (μL)	Volume 10 mM $K_{50}(+)$ (μL)	Volume 2 M NaCl added (μL)	Volume water added (μL)
1	0.500	6.0	6.0	0.0	108.0
2	0.500	6.0	6.0	1.5	106.5
3	0.500	6.0	6.0	3.0	105.0
4	0.500	6.0	6.0	4.5	103.5
5	0.500	6.0	6.0	6.0	102.0
6	0.500	6.0	6.0	9.0	99.0
7	0.500	6.0	6.0	12.0	96.0
8	0.500	6.0	6.0	18.0	90.0
9	0.500	6.0	6.0	21.0	87.0
10	0.500	6.0	6.0	24.0	84.0
11	0.500	6.0	6.0	27.0	81.0
12	0.500	6.0	6.0	30.0	78.0
13	0.500	6.0	6.0	36.0	72.0
14	0.500	6.0	6.0	42.0	66.0
15	0.500	6.0	6.0	48.0	60.0
16	0.500	6.0	6.0	54.0	54.0
Blank	–	0.0	0.0	0.0	120.0

Components were added from right to left as outlined in the protocol. The final monomer concentration is 1 mM.

from that of a blank solution at the same salt/buffer concentration, but in the absence of polymer. In our experience, samples should be prepared at a final concentration of at least 1 mM (with respect to the total number of monomers), though this threshold concentration is a function of the path length through the sample.

To facilitate the preparation of fully equilibrated coacervate samples, we recommend that any salt, buffer, and excess water are combined first, followed by the addition of one of the polymers. It is then important to ensure that the sample is well mixed (e.g., vortexing for 5–10 s) before

the second polymer is added, and that the sample is mixed again after the addition of the second polymer. It is also possible to prepare the polymer stock solutions at a specified concentration of salt/buffer, thereby eliminating the need to add these components separately, though this approach is less flexible in terms of adjusting experimental parameters. Once samples have been prepared, they should be mixed well and transferred to a well plate or cuvette for turbidity analysis. An example turbidity result for a stoichiometry experiment between poly(L-lysine) and poly(D,L-glutamate), degree of polymerization $N = 50$, pH 7.0 is shown in Fig. 2A. The coacervate samples, as formed, should be a dispersion of droplets that gives the sample a cloudy and possibly opalescent appearance. At this point, the time between sample preparation and analysis is an important consideration, as the coacervate droplets can coalesce and settle over time and thus give variable turbidity readings. Generally, the turbidity signal should not be sensitive to differences of a few minutes, though this time scale can vary significantly based on the identity of the polymer system and the solution conditions.

While all experimental results should be replicated in order to ensure reproducibility (i.e., "technical" replicates), we also recommend that samples be prepared in such a way that each sample can be split and analyzed separately (a repeat measurement of the sample, similar to a "biological" replicate). The use of three replicates/repeats will allow for the statistical analysis of the resulting data. In terms of sample preparation, the total volume of sample prepared for a repeated measurement should be $>3\times$ the volume

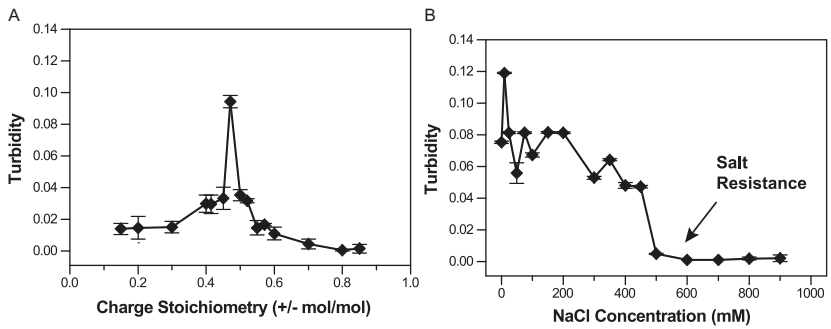

Fig. 2 Turbidity data from (A) stoichiometry experiments involving poly(L-lysine) and poly(D,L-glutamate) with a degree of polymerization N = 50, pH 7.0 with no added buffer and (B) salt resistance experiments as a function of increasing NaCl concentration. The final monomer concentration was 1 mM. Lines connecting the data points are a guide for the eye.

needed for the three individual samples. For example, 35 μL of sample is needed for a turbidity measurement using a 384-well plate. However, to ensure that sufficient sample volume is available for pipetting, a total sample volume of 120 μL might be prepared.

After turbidimetry, samples should be inspected visually using an optical microscope. Standard brightfield microscopy with a 40 × objective is typically sufficient for this procedure, though more advanced techniques such as phase contrast or differential interference contrast (DIC) can enhance the ability to visualize samples. For samples prepared at low polymer concentration, it may be difficult to distinguish very small droplets. The size of these coacervate droplets can be increased either by increasing the polymer concentration present in the sample, or by allowing the sample more time for the droplets to coalesce. The main goals in visualizing coacervate samples are to confirm the liquid vs. solid nature of the resulting materials, and provide secondary confirmation of trends (e.g., the presence or absence of coacervates) suggested via turbidity. Coacervate droplets should appear as circular/spherical structures either floating in solution or adhered onto a surface, whereas solid precipitation typically appears as fractal aggregates (Fig. 3).

An important consideration in the preparation of coacervates is whether they are fully equilibrated. This question can be answered by testing whether or not the results of an experiment are sensitive to the order of polymer addition.

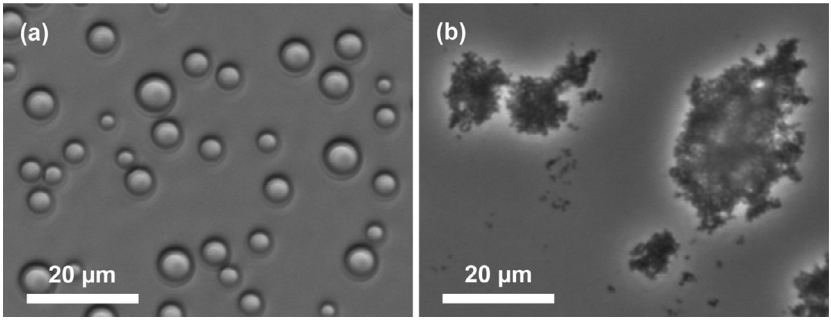

Fig. 3 Optical micrographs of (A) liquid complex coacervate droplets of poly(L-lysine) and poly(D,L-glutamate), and (B) fractal solid precipitates resulting from the interaction of poly(L-lysine) and poly(L-glutamate). All samples were prepared using polymers with degree of polymerization $N = 100$ at a total monomer concentration of 6 mM in 100 mM NaCl, pH 7.0.

4.3 Polymer-polymer salt resistance experiments

The goal of salt resistance experiments is to identify the concentration of salt (for a given total polymer concentration and stoichiometric ratio) above which phase separation is no longer observed. This provides information on the location of the binodal curve, and informs the design of experimental procedures where dissolution of the coacervate phase is needed. The magnitude of the salt resistance is dependent upon the length and identity of the polymers, the choice of salt, the solution pH, etc. Generally speaking, increases in polymer length, hydrophobicity, and charge density will result in higher values of the salt resistance at the same polymer concentration.

In designing a salt resistance experiment for a new polymer, it may be necessary to perform a screening-level experiment to identify the general range of salt concentrations over which the experiment should be performed. Generally, the salt resistance can be identified as a clear decrease in the turbidity signal with increasing salt concentration. However, it is useful to combine turbidimetry measurements with direct visualization of the samples via optical microscopy to confirm results. An example of salt resistance data for the system of poly(L-lysine) and poly(D,L-glutamate) degree of polymerization $N = 50$, pH 7.0 is shown in Fig. 2B.

A general step-by-step protocol for these polymer-only experiments is given below.

4.4 Experimental protocol for coacervate samples (no protein)

1. Set up microcentrifuge tubes for each sample and a blank, labeling appropriately
2. Pipette the appropriate amount of water into each tube (as needed)
3. Pipette the appropriate amount of buffer solution into each tube (as needed)
4. Pipette the appropriate amount of salt solution into each tube (as needed)
5. Pipette the appropriate amount of the first polyelectrolyte solution into each tube
6. Vortex each tube for 5–10 s
7. Pipette the appropriate amount of the second polyelectrolyte solution into each tube, vortexing for 5–10 s immediately after each addition
8. Transfer aliquots of each sample to the well plate or cuvette for turbidity analysis
9. Inspect each sample via optical microscopy

4.5 Polymer-polymer-protein stoichiometry experiments

The design of a stoichiometry experiment for a system that combines protein in the presence of a polycation and polyanion varies only slightly in design and intent. While more extensive experiments that vary the relative amounts of each polymer and the quantity of protein can be performed to map out the complete phase behavior of this more complex system, simpler experiments that consider the effect of polymer charge stoichiometry in the presence of a constant level of protein can also be performed (see Table 3 for an example recipe). Here, we will discuss the design of these

Table 3 Sample preparation for complexation between poly(L-lysine) (K_{50}) and poly(D,L-glutamate) (E_{50}), degree of polymerization $N = 50$, in 10 mM HEPES buffer pH 7.0 with bovine serum albumin (BSA).

	Charge fraction $K_{50}(+)$	Volume 10 mM $E_{50}(-)$ (μL)	Volume 10 mM $K_{50}(+)$ (μL)	Volume 2 mg/mL BSA (−) added (μL)	Volume 0.5 M HEPES added (μL)	Volume water added (μL)
1	0.100	151.2	16.8	6.0	4.80	61.2
2	0.200	134.4	33.6	6.0	4.80	61.2
3	0.300	117.6	50.4	6.0	4.80	61.2
4	0.400	100.8	67.2	6.0	4.80	61.2
5	0.425	96.6	71.4	6.0	4.80	61.2
6	0.450	92.4	75.6	6.0	4.80	61.2
7	0.475	88.2	79.8	6.0	4.80	61.2
8	0.500	84.0	84.0	6.0	4.80	61.2
9	0.525	79.8	88.2	6.0	4.80	61.2
10	0.550	75.6	92.4	6.0	4.80	61.2
11	0.575	71.4	96.6	6.0	4.80	61.2
12	0.600	67.2	100.8	6.0	4.80	61.2
13	0.700	50.4	117.6	6.0	4.80	61.2
14	0.800	33.6	134.4	6.0	4.80	61.2
15	0.900	16.8	151.2	6.0	4.80	61.2
Blank	0.000	0.0	0.0	0.0	4.80	235.2

Components were added from right to left as outlined in the protocol. The final monomer concentration is 7 mM and the final protein concentration is 50 μg/mL.

simpler experiments and how the addition of a protein as a third charged macromolecule can alter the phase behavior of the system.

Our initial stoichiometry experiments with just the two-polymer system served to identify the composition corresponding to maximum coacervate yield, corresponding to a charge-neutral mixture of the two polymers. However, the addition of a charged protein would be expected to shift this optimal condition. As can be seen in Fig. 4A, the addition of negatively-charged bovine serum albumin (BSA) to a mixture of poly(L-lysine) and poly(D,L-glutamate) degree of polymerization $N = 50$, in 10 mM HEPES, pH 7.0 results in a shift in the resulting turbidity signal to higher mole fractions of the polycation. A shift in the opposite direction, to "net negative" conditions would be expected for positively-charged proteins (Blocher McTigue & Perry, 2019; Lindhoud & Claessens, 2016; Lindhoud, Norde, & Cohen Stuart, 2009).

As for the two-polymer system, it is important to determine whether the order of mixing has any effect on the resulting coacervates.

4.6 Polymer-polymer-protein salt resistance experiments

Salt resistance experiments can also be performed for samples including proteins. However, most proteins would be expected to have a lower charge content and charge density than the associated polymers. As such, it is a

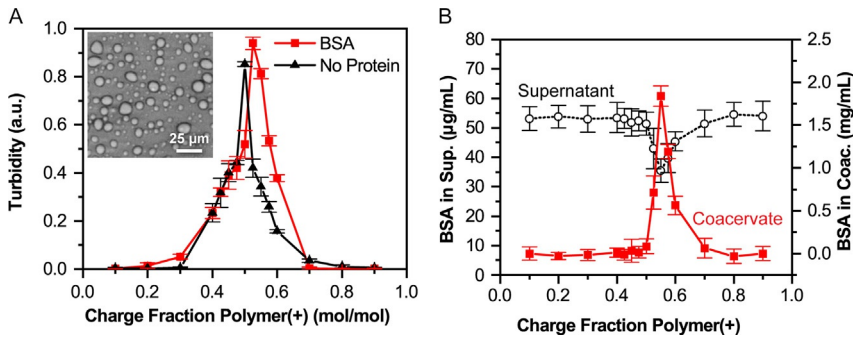

Fig. 4 (A) Turbidity data from stoichiometry experiments involving poly(L-lysine) and poly(D,L-glutamate) with a degree of polymerization $N = 50$ (black) and for the same system with the anionic protein bovine serum albumin (BSA) (red) in 10 mM HEPES, pH 7.0. The inset optical micrograph shows the formation of coacervate droplets with BSA. (B) The corresponding concentration of protein in the supernatant (black) and coacervate (red) phases, as determined using a Bradford assay. *Blocher McTigue, W. C., Perry, S. L. (2019). Design rules for encapsulating proteins into complex coacervates.* Soft Matter, 15, *3089–3103. Reproduced by permission of The Royal Society of Chemistry.*

reasonable assumption that the salt resistance of the three-macromolecule system should be lower than that of the polymer-only system.

A general step-by-step protocol for these polymer-polymer-protein experiments is given below.

4.7 Experimental protocol for coacervate samples (with protein)

1. Set up microcentrifuge tubes for each sample and a blank, labeling appropriately
2. Pipette the appropriate amount of water into each tube (as needed)
3. Pipette the appropriate amount of buffer solution into each tube (as needed)
4. Pipette the appropriate amount of salt solution into each tube (as needed)
5. Pipette the appropriate amount of the first polyelectrolyte solution into each tube
6. Vortex each tube for 5–10 s
7. Pipette the appropriate amount of the protein solution into each tube, vortexing for 5–10 s immediately after each addition
8. Pipette the appropriate amount of the second polyelectrolyte solution into each tube, vortexing for 5–10 s immediately after each addition
9. Transfer aliquots of each sample to the well plate or cuvette for turbidity analysis
10. Inspect each sample via optical microscopy

4.8 Quantifying protein incorporation into complex coacervates

While turbidity and optical microscopy can be used to determine whether complexation has occurred or not, these measurements do not provide information on the incorporation of protein into the coacervate phase. Instead, separate measures of the protein concentration in the coacervate and supernatant phases must be made, along with a determination of the volume of each phase.

Once the concentrations for both the coacervate and supernatant phases are known, several other parameters may be determined. The first is the encapsulation efficiency (*EE*), which is the percentage of cargo (by mass) sequestered, in this case, by complex coacervates. Measuring the supernatant volume and multiplying by the concentration of protein in the supernatant phase gives the mass of cargo in the supernatant. Subtracting this mass from

the total mass of protein added to the system during sample preparation allows for calculation of the mass of protein in the coacervate phase. These masses can then be used to calculate the encapsulation efficiency:

$$EE = \frac{m_{coac.\ protein}}{m_{total\ protein}} x100\% \tag{1}$$

A partition coefficient, on the other hand, is typically defined as the ratio of the concentration of protein in the dense coacervate phase over the concentration of the cargo in the dilute phase, written as:

$$K = \frac{\left[cargo_{coac.\ protein}\right]}{\left[cargo_{sup.\ protein}\right]} \tag{2}$$

Finally, loading or loading capacity is the amount of protein in the coacervate compared to the total mass of the coacervate, i.e., it describes what fraction of the coacervate phase is comprised of the cargo:

$$LC = \frac{m_{coac.\ protien}}{m_{coac.\ total}} x100\% \tag{3}$$

Below, we will detail strategies for assaying the protein concentration in coacervate samples using a colorimetric Bradford assay, and via direct measurement of protein absorbance.

4.9 Bradford assay

The protein quantification experiments described here are intended to be run in parallel with a stoichiometry-type experiment, as described above, with half of the total sample volume used for turbidity experiments, and the other half used for protein quantification. As in the case of turbidity experiments, it is important to measure both repeat and replicate samples in order to allow for statistical analysis of the results.

The Coomassie brilliant blue G-250 dye used in the Bradford assay is typically described as interacting with basic amino acids in hydrophobic pockets, but primarily responds to arginine residues, as well as histidine, tryptophan, tyrosine, and phenylalanine to a lesser extent (Bio-Rad Laboratories, n.d.; Olson & Markwell, 2007; Stoscheck, 1990). Typically, users buy a kit that may come with protein standards (e.g., bovine serum albumin, BSA) to aid in the creation of a calibration curve. However, individual proteins interact differently with the Coomassie dye, based on their amino acid sequence. Therefore, we recommend creating calibration curves

directly with the protein of interest. Furthermore, all calibration curves must be prepared at the solution conditions (i.e., pH, salt concentration, etc.) expected in the final sample. One consequence of this is that separate calibration curves are required for supernatant samples, which can be measured directly, and coacervate samples, which must be performed at a higher salt concentration in order to dismantle the coacervate (Fig. 5).

In addition to considering the specific interactions of the Coomassie dye with the protein at different solution conditions, it is critical to determine the potential background signal that might result from the dye interacting with the polymers used in the coacervate. While the interaction of the dye with poly(L-lysine) and poly(D,L-glutamate) has been shown to be minimal (Blocher McTigue & Perry, 2019), much stronger interactions occur when more hydrophobic polymers such as poly(styrene sulfonate) (PSS), poly(diallyldimethylammonium chloride) (PDADMAC), and methacrylate-based polyelectrolytes. The interaction between polymer and dye can be tested by mixing a 1:1 volume ratio of the dye with a solution of polymer at the concentration intended for use in experiments. Qualitatively, a strong interaction between the dye and the polymers can be observed visually as a color change from brackish-brown to blue. Quantitatively, it is important to consider whether the level of background signal resulting from the polymers in the coacervate will swamp the potential absorbance signal from the protein by itself. This comparison can be done via an absorbance measurement at 595 nm. While it is possible to perform a background subtraction to account for signal associated with the polyelectrolytes, this correction can become complicated if the concentration of each of the polymers varies across different samples.

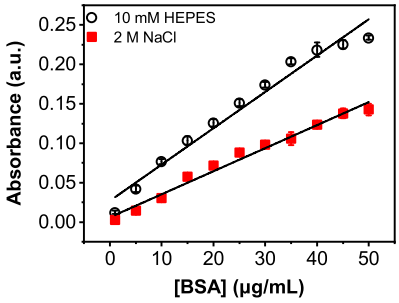

Fig. 5 Standard curves for BSA for a Bradford assay in 10 mM HEPES pH 7.0 (black open circles) with a 1:1 dye to sample ratio and 2 M NaCl (red squares) with a 1:1 dye to sample ratio corresponding to the supernatant and coacervate phases. The black lines represent linear fits.

The linear range of the Bradford assay is a function of the specific interaction of the protein with the Coomassie dye, and the volumetric scale (and thus the absorbance path length) at which the experiment is performed. Different scale protocols have been developed for the Bradford assay depending on the desired sample volumes and the range of concentrations. The main difference in the protocols is the ratio of Coomassie dye solution to protein sample. For example, the "standard" Bradford protocol uses a 50:1 ratio of dye to sample, and has a typical range of ~125–1000 μg/mL. In contrast, the "micro assay" uses a 1:1 ratio of dye to sample and has a linear range of approximately 1–10 μg/mL (Bio-Rad Laboratories, n.d.). These ratios, as well as the sample path length can be tuned to optimize a protocol for a specific protein target and/or solution condition. For more information on the Bradford assay, we encourage readers to refer to Bio-Rad Laboratories (n.d.) and Olson and Markwell (2007).

For the example data shown in Fig. 4 and Table 3, we assayed the uptake of bovine serum albumin (BSA) into coacervates formed from poly(L-lysine) and poly(D,L-glutamate) with a degree of polymerization $N = 50$, in 10 mM HEPES, pH 7.0. The experiment tested the incorporation of 50 μg/mL BSA as a function of the charge stoichiometry of the two polymers. A "micro assay" style Bradford assay was used to quantify the protein concentration in both the coacervate and the supernatant phases. Samples were prepared at a total volume of 240 μL, 105 μL of which was used for turbidity measurements (3 repeat samples of 35 μL each), and 115 μL of which was used for protein quantification. After separating the coacervate and supernatant, protocols were developed separately for the two phases.

Having measured the total volume of the supernatant for each sample to facilitate future mass balance calculations, 115 μL of supernatant was then aliquoted into a clean microcentrifuge tube and combined with an equal volume (115 μL) of 1 × Coomassie dye. Three repeat aliquots of 35 μL each were then pipetted into a 384-well plate for absorbance measurements. The absorbance data were converted to concentration values using a standard curve with samples prepared in 10 mM HEPES, pH 7.0.

For the coacervate samples, visual inspection after centrifugation had determined that the volume of coacervate was very small (~0–2.2 μL). We then added 70 μL of 2.0 M NaCl to disassemble the coacervate. This sample was then mixed with an equal volume (70 μL) of 1 × Coomassie dye. For these samples, we chose to neglect the volume of our coacervate in subsequent concentration calculations as an error of ~0–2.2 μL represents

a ~3% volume error. Three repeat aliquots of 35 μL each were then pipetted into a 384-well plate for absorbance measurements, as above. The absorbance data for coacervate samples were converted to concentration using a standard curve with samples prepared at a concentration of 2 M NaCl.

The data in Fig. 4A show a strong peak in the turbidity at a mole fraction of polycation of approximately 0.525. This peak in the turbidity data corresponds directly with a strong increase in the concentration of protein present in the coacervate phase (to nearly 2.0 mg/mL, or 2000 μg/mL), and a corresponding decrease in the protein from the supernatant (Fig. 4B). In contrast, for samples at the extremes of the stoichiometric range where no phase separation occurred, we recovered the expected value of 50 μg/mL BSA that was input into the system.

4.10 Experimental protocol for protein quantification using the Bradford assay

1. Perform steps 1–10 as described above for "Experimental protocol for coacervate samples (with protein)." Samples should be prepared at a volume scale 2 × the quantity needed for a turbidity experiment
2. Centrifuge samples to phase separate the coacervate and supernatant phases for 20 min at 14,000 rpm (18,800 × *g*) at 15 °C
3. Use a pipette to transfer the supernatant into a new microcentrifuge tube carefully, noting the volume

   In many instances, such as the samples described in Table 3, it is difficult to directly obtain accurate measurements of coacervate volumes that can be on the order of ~1 μL. To circumvent this issue, we can estimate this volume by subtracting the measured value of the supernatant volume from the measured total sample volume after formulation, but before centrifugation.
4. Pipette a sufficient volume of a concentrated stock solution of salt (e.g., 2 M NaCl) to cause the dissolution of the coacervate phase and create a large enough volume sample to run multiple aliquots for the Bradford assay. The necessary concentration of salt can be determined by a salt resistance experiment, as described above
5. Pipette the necessary volume of Coomassie dye to the supernatant and coacervate samples
6. Vortex each tube for 5–10 s
7. Transfer aliquots of the supernatant and coacervate samples into to the well plate or cuvette, taking care to avoid and/or remove bubbles

8. Measure the absorbance of the samples and a blank at 595 nm
9. Convert the measured absorbance values to protein concentration using the appropriate standard curve

4.11 Utilizing absorbance at 280 nm

While the Bradford assay is performed using a colorimetric readout, measuring absorbance at 280 nm (A280) requires special consideration. Many standard well plates and disposable cuvettes may not be suited for this method as many plastics absorb in the UV. Specialized plastic cuvettes, quartz cuvettes, and small volume absorbance setups such as the NanoDrop or Take3 should be used for these measurements.

The linear range of concentrations measurable by absorbance at 280 nm generally extends from ~20 to ~3000 μg/mL (Simonian, 2002). However, the specific measurable range will be a function of the extinction coefficient for a given protein, in tandem with potential background interference from other components of the solution, as well as the path length of the sample. For example, the standard range for the small volume NanoDrop system is between 0.1 and 400 mg/mL for BSA, which has an extinction coefficient of 43,824 M^{-1} cm^{-1}, assuming a molecular weight of 66.4 kDa (Thermo Scientific, 2010). However, this range can be heavily influenced by the presence of other molecules present in solution, such as salt, buffer, surfactants, etc. Table 3 lists the maximum allowable concentration for a range of common chemicals related to these absorbance measurements.

In the specific context of complex coacervate samples, it is important to test whether or not the polyelectrolytes used to form the coacervate absorb at 280 nm. While it is possible to perform a background subtraction to account for signal associated with the polyelectrolytes, this correction can become complicated if the concentration of each of the polymers varies across different samples.

In each case, there is a known path length to use for l in Beer's equation:

$$A = c\varepsilon l \tag{4}$$

The extinction coefficient can be found using programs such as ProtParam or looking into the literature (Gasteiger et al., 2005). If there is no known extinction coefficient and no sequence, a standard assumption is that an absorbance reading of 1.0 is equal to 1 mg/mL based on a 0.1% or 1 mg/mL protein concentration producing an absorbance at 280 nm of 1.0 with a path length of 10 mm or 1 cm (Stoscheck, 1990).

In general, the molar extinction coefficient (in units of $M^{-1}\,cm^{-1}$) is approximated as:

$$\varepsilon = 5500W + 1490Y + 125C \tag{5}$$

where W is the number of tryptophans, Y is the number of tyrosines, and C is the number of cysteines in the protein sequence. Each number before the amino acids is the molar absorptivity at 280 nm for that residue. It is noteworthy that extinction coefficients are frequently reported using a range of different units, thus knowing the conversions is sometimes necessary for analysis. To convert to a percent extinction coefficient, which has units of $(g/100\ mL)^{-1}\,cm^{-1}$, the formula is:

$$\varepsilon_{1\%} = \frac{10\varepsilon}{MW} \tag{6}$$

where MW is the molecular weight of the protein. Another common form is the 0.1% extinction coefficient and has units of $(mg/mL)^{-1}\,cm^{-1}$. Converting to the 0.1% extinction coefficient follows:

$$\varepsilon_{0.1\%} = \frac{\varepsilon_{\%}}{10} = \frac{\varepsilon}{MW} \tag{7}$$

The use of a program to calculate protein concentration using absorbance at 280 nm may have correction calculations, appropriate reading of the literature and user guides will help determine such corrections. If it is suspected that the protein sample has nucleic contamination, Eq. 8 may be used for an approximate determination: (Olson & Markwell, 2007; Stoscheck, 1990):

$$[protein](mg/mL) = (1.55\ x\ A_{280}) - (0.76\ x\ A_{260}) \tag{8}$$

However, a potentially simpler method for protein quantification at 280 nm is to create a standard curve of the protein. This is useful for systems that employ various buffer conditions that may affect results and does not require a NanoDrop program or use of an extinction coefficient. Standard curves are made by preparing known sample concentrations at desired conditions and running them at 280 nm, subtracting out a blank. It is good for scientists, however, to understand where the math comes from if a NanoDrop or similar system is used. Note that many of these systems have additional blank subtraction and correction procedures built in.

4.11.1 Experimental protocol for protein quantification using A280

1. Perform steps 1–4 as described above for the Bradford protocol
2. Pipette an aliquot of known volume for absorbance measurements
   a. A Take3 or NanoDrop system allow for the use of ~2 μL with a known path length
   b. A UV-compatible cuvette can be used with a larger sample volume
3. Measure the absorbance of the samples and a blank at 280 nm
4. Convert the measured absorbance values to protein concentration using the appropriate standard curve
   a. Take3/NanoDrop have built in programs for 280 nm and are recommended for specific moieties, such as BSA and IgG, with appropriate extinction coefficients
   b. A standard curve may be used to determine protein concentration if extinction coefficient is unknown or the extinction coefficient can be calculated via code or from another program such as ProtParam (Gasteiger et al., 2005).

4.12 Standard curves

For all of the methods described, it is necessary to create a standard curve to determine the concentration of protein from the measured absorbance signal. While BSA is commonly used as a protein standard to generate a "universal" set of standard curves, the colorimetric signal from the Coomassie dye and/or the absorbance at 280 nm can vary widely from protein to protein, and as a function of solution conditions. Thus, we advise the creation of a standard curve for each protein at every set of experimental conditions used. Table 4 outlines limits for several common buffers, salts, etc., for the Bradford assay and 280 nm (Stoscheck, 1990). Generally speaking, measurements at 280 nm are sensitive to molecules that have double bonds between carbons or carbon and oxygen (Stoscheck, 1990), while the Bradford assay does not tolerate high concentrations of detergents (Olson & Markwell, 2007).

Based on the various limits of detection for the different methods and the anticipated concentrations of proteins, standard curves should be prepared at the relevant solution conditions for the supernatant and coacervate samples. It is recommended that standard curves have at least five points and completely span the range of interest. Example standard curves corresponding to the supernatant and coacervate samples from Fig. 4 are shown in Fig. 5.

Table 4 Concentration limits for protein assays using Coomassie dye and absorbance at 280 nm.

Concentration limits for protein assays[a]

Substance[b]		Dye[c]	280 nm[d]
Acids and bases			
	HCl	0.1 M	>1 M
	NaOH	0.1 M	>1 M
	PCA		10%
	TCA		10%
Buffers			
	Acetate	0.6 M	0.1 M
	Ammonium sulfate	1 M	>50%
	Citrate	50 mM	5%
	Glycine	0.1 M	1 M
	HEPES	100 mM	
	Phosphate	2 M	1 M
	Tris	2 M	0.5 M
Detergents			
	Brij 35		1%
	CHAPS		10%
	Deoxycholate	0.25%	0.30%
	Digitonin		10%
	Lubrol PX		10%
	Octylglucoside		10%
	SDS	0.10%	0.10%
	Triton X-100	0.10%	0.02%
	Triton X-100(R)		>10%
	Tween 20		0.30%
Reductants			
	Dithiothreitol	1 M	3 mM
	2-Mercaptoethanol	1 M	10 mM

Table 4 Concentration limits for protein assays using Coomassie dye and absorbance at 280 nm.—cont'd

Concentration limits for protein assays[a]

Substance[b]		Dye[c]	280 nm[d]
Miscellaneous			
	DNA/RNA	0.25 mg	1 μg
	DMSO		20%
	EDTA	0.1 M	30 mM
	Glycerol	100%	40%
	KCl	1 M	100 mM
	NaCl	5 M	>1 M
	Sucrose	1 M	2 M
	Urea	6 M	>1 M

[a]This table is a guide. Test buffer mixtures as described in the text. Values preceded by (<) or (>) symbols indicate that that tolerable limit for the chemical is unknown but is, respectively, less than or greater than the amount shown. Blank spaces indicate data were unavailable.
[b]PCA, Perchloric acid; TCA, trichloroacetic acid; HEPES, *N*-2-hydroxyehtylpiperazine-*N*′-2-ethanesulfonic acid; CHAPS, 3-[(3-cholamidopropyl)dimethylammino]propanesulfonic acid; SDS, sodium dodecyl sulfate; (R), reduced; DMSO, dimethyl sulfoxide; EDTA ehtylenediamine-tetraacetic acid.
[c]Values indicate the concentration of the chemical in a 25 μL sample.
[d]Values indicate the final concentration of the chemical which does not produce an absorbance of 0.5 compared to an equivalent water blank.
Values adapted from Olson, B. J. S. C., Markwell, J. (2007). *Assays for determination of protein concentration* (pp. Unit3.4–3.4.29). Hoboken, NJ: John Wiley & Sons, Inc., Vol. Chapter 3.

The best practice is to make new curves for every new cargo as they vary from protein to protein, as seen comparing the curves from Fig. 5 and Fig. 6A. Additionally, varying the ratio of dye to sample can change the linear range of a protein. In the case of hen egg white lysozyme (HEWL), a ratio of two parts dye to one part sample is used to extend the range to 50 μg/mL (Fig. 6A). If the same ratio was used as for BSA in Fig. 5, the result is no longer linear (Fig. 6B). The more dye added, the longer the linear range, this also allows for smaller sample volumes.

Table 5 shows an example recipe for a standard curve is outlined in Figs. 5 and 6 to create a curve that would place the target concentration in the middle of the range at pH 7.0 in 10 mM HEPES. The goal is to create a linear curve over the desired range of concentrations using the Bradford. A curve for both the supernatant and coacervate phases is required.

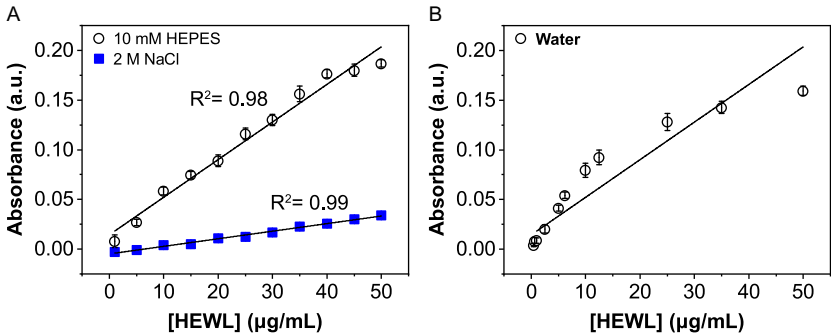

Fig. 6 (A) Standard curves for HEWL for a Bradford assay in 10 mM HEPES pH 7.0 (black open circles) with a 2:1 dye to sample ratio and 2 M NaCl (blue squares) with a 1:1 dye to sample ratio corresponding to the supernatant and coacervate phases. (B) Standard curve for HEWL for a Bradford assay in water with a 1:1 dye to sample ratio, which shows a shorter linear range. The black lines represent linear fits to the data.

Table 5 Standard curve example table for bovine serum albumin (BSA) or hen egg white lysozyme (HEWL) for the supernatant phase.

Point	(Protein) (μg/mL)	0.2 mg/mL protein (μL)	0.5 M HEPES (μL)	Water (μL)
1	1	0.6	2.4	117.0
2	5	3.0	2.4	114.6
3	10	6.0	2.4	111.6
4	15	9.0	2.4	108.6
5	20	12.0	2.4	105.6
6	25	15.0	2.4	102.6
7	30	18.0	2.4	99.6
8	35	21.0	2.4	96.6
9	40	24.0	2.4	93.6
10	45	27.0	2.4	90.6
11	50	30.0	2.4	87.6
12	55	33.0	2.4	84.6
13	60	36.0	2.4	81.6
14	65	39.0	2.4	78.6
15	70	42.0	2.4	75.6
Blank	0	0	2.4	117.6

Total solution volume is 120 μL and can be used for a 96 (120 μL/well) or 384-well plate (35 μL/well ×3).

The supernatant will have the conditions set by sample preparation, while the coacervate phase will necessitate whatever conditions are used to dismantle the dense phase, i.e., 2M NaCl. To convert Table 5 from samples related to the supernatant phase to those from the coacervate phase, replace the total volume of buffer (HEPES) and water with an equal amount of salt.

5. Analysis and statistics

To facilitate statistical analysis, repeat samples and replicate experiments should be performed at least three times. A standard *t*-test or ANOVA may be used for comparison between assay results.

Moving beyond raw data to calculated values such as the concentration of protein in the coacervate phase, the encapsulation efficiency, partitioning, etc., require propagation of error. Furthermore, propagation of error should be considered when performing baseline subtraction. To obtain an equation for the propagated error use:

$$\delta R = \sqrt{\left(\frac{\partial R}{\partial x}\delta x\right)^2 + \left(\frac{\partial R}{\partial y}\delta y\right)^2 + \ldots} \tag{9}$$

where R is the parameter whose error is being calculated and is a function of x, y, etc. The partial derivative of R for a specific independent variable is multiplied by the error of that variable and the whole quantity squared. This is done for each variable for which R is dependent and summed together. Finally, the square root of the summation is taken and that is the error for R. For example, the propagated error associated with performing a baseline subtraction between averaged values of the sample and baseline absorbance is:

$$\delta A_{avg,b} = \sqrt{\left(\frac{\partial}{\partial b}\left(A_{avg} - b\right)\delta b\right)^2 + \left(\frac{\partial}{\partial A_{avg}}\left(A_{avg} - b\right)\delta A_{avg}\right)^2} \tag{10}$$

This type of calculation should be performed for each mathematical manipulation performed during data analysis. When using a standard curve, there is an associated error with the fit, which should be included using error propagation. This error can be determined by using Eq. 9.

6. Summary

Complex coacervates are a novel materials platform for the encapsulation and delivery of a wide range of materials, including proteins. We have discussed strategies for understanding the phase behavior associated with the coacervation of polymeric systems in the absence and presence of protein, along with methods for measuring the concentration of protein in coacervate samples. Here we have shown that it is possible to use established methods and adapt them to coacervate systems for protein analysis.

Acknowledgments

W.C.B.M. was supported by a Fellowship from the Soft Materials for Life Sciences National Research Traineeship Program #NRT-1545399. We would also like to thank PPG for funding support of W.C.B.M. through a grant to the Department of Chemical Engineering at the University of Massachusetts Amherst.

References

Bio-Rad Laboratories. n.d. Quick Start™ Bradford protein assay; pp 1–36.

Black, K. A., Priftis, D., Perry, S. L., Yip, J., Byun, W. Y., & Tirrell, M. (2014). Protein encapsulation via polypeptide complex coacervation. *ACS Macro Letters*, *3*(10), 1088–1091. https://doi.org/10.1021/mz500529v.

Blocher McTigue, W. C., & Perry, S. L. (2019). Design rules for encapsulating proteins into complex coacervates. *Soft Matter*, *15*, 3089–3103. https://doi.org/10.1039/C9SM00372J.

Bourganis, V., Karamanidou, T., Kammona, O., & Kiparissides, C. (2017). Polyelectrolyte complexes as prospective carriers for the oral delivery of protein therapeutics. *European Journal of Pharmaceutics and Biopharmaceutics*, *111*, 44–60. https://doi.org/10.1016/j.ejpb.2016.11.005.

Carvalho, I. T., Estevinho, B. N., & Santos, L. (2016). Application of microencapsulated essential oils in cosmetic and personal healthcare products—A review. *International Journal of Cosmetic Science*, *38*(2), 109–119. https://doi.org/10.1111/ics.12232.

Chang, L.-W., Lytle, T. K., Radhakrishna, M., Madinya, J. J., Vélez, J., Sing, C. E., et al. (2017). Sequence and entropy-based control of complex coacervates. *Nature Communications*, *8*, 1273. https://doi.org/10.1038/s41467-017-01249-1.

Chapeau, A.-L., Bertrand, N., Briard-Bion, V., Hamon, P., Poncelet, D., & Bouhallab, S. (2017). Coacervates of whey proteins to protect and improve the oral delivery of a bioactive molecule. *Journal of Functional Foods*, *38*, 197–204. https://doi.org/10.1016/j.jff.2017.09.009.

Chollakup, R., Beck, J. B., Dirnberger, K., Tirrell, M., & Eisenbach, C. D. (2013). Polyelectrolyte molecular weight and salt effects on the phase behavior and coacervation of aqueous solutions of poly(acrylic acid) sodium salt and poly(allylamine) hydrochloride. *Macromolecules*, *46*(6), 2376–2390. https://doi.org/10.1021/ma202172q.

Chollakup, R., Smitthipong, W., Eisenbach, C. D., & Tirrell, M. (2010). Phase behavior and coacervation of aqueous poly(acrylic acid)−poly(allylamine) solutions. *Macromolecules*, *43*(5), 2518–2528. https://doi.org/10.1021/ma902144k.

Comert, F., & Dubin, P. L. (2017). Liquid-liquid and liquid-solid phase separation in protein-polyelectrolyte systems. *Advances in Colloid and Interface Science*, *239*, 213–217. https://doi.org/10.1016/j.cis.2016.08.005.

Comert, F., Malanowski, A. J., Azarikia, F., & Dubin, P. L. (2016). Coacervation and precipitation in polysaccharide-protein systems. *Soft Matter*, *12*, 4154–4161. https://doi.org/10.1039/C6SM00044D.

Cooper, C. L., Dubin, P. L., Kayitmazer, A. B., & Turksen, S. (2005). Polyelectrolyte–protein complexes. *Current Opinion in Colloid & Interface Science*, *10*(1–2), 52–78. https://doi.org/10.1016/j.cocis.2005.05.007.

Cummings, C. S., & Obermeyer, A. C. (2018). Phase separation behavior of supercharged proteins and polyelectrolytes. *Biochemistry*, *57*(3), 314–323. https://doi.org/10.1021/acs.biochem.7b00990.

Gasteiger, E., Hoogland, C., Gattiker, A., Duvaud, S., Wilkins, M. R., Appel, R. D., et al. (2005). In J. M. Walker (Ed.), *The Proteomics Protocols Handbook* (pp. 571–607). Humana Press.

Johnson, N. R., & Wang, Y. (2013). Controlled delivery of heparin-binding EGF-like growth factor yields fast and comprehensive wound healing. *Journal of Controlled Release*, *166*(2), 124–129. https://doi.org/10.1016/j.jconrel.2012.11.004.

Johnson, N. R., & Wang, Y. (2014). Coacervate delivery systems for proteins and small molecule drugs. *Expert Opinion on Drug Delivery*, *11*(12), 1829–1832. https://doi.org/10.1517/17425247.2014.941355.

Kaibara, K., Okazaki, T., Bohidar, H. B., & Dubin, P. L. (2000). pH-induced coacervation in complexes of bovine serum albumin and cationic polyelectrolytes. *Biomacromolecules*, *1*(1), 100–107. https://doi.org/10.1021/bm990006k.

Kishimura, A., Koide, A., Osada, K., Yamasaki, Y., & Kataoka, K. (2007). Encapsulation of myoglobin in PEGylated polyion complex vesicles made from a pair of oppositely charged block ionomers: A physiologically available oxygen carrier. *Angewandte Chemie, International Edition*, *46*(32), 6085–6088. https://doi.org/10.1002/anie.200701776.

Kuo, C.-H., Leon, L., Chung, E. J., Huang, R.-T., Sontag, T. J., Reardon, C. A., et al. (2014). Inhibition of atherosclerosis-promoting microRNAs via targeted polyelectrolyte complex micelles. *Journal of Materials Chemistry B*, *2*, 8142–8153. https://doi.org/10.1039/C4TB00977K.

Li, L., Srivastava, S., Andreev, M., Marciel, A. B., de Pablo, J. J., & Tirrell, M. V. (2018). Phase behavior and salt partitioning in polyelectrolyte complex coacervates. *Macromolecules*, *51*(8), 2988–2995. https://doi.org/10.1021/acs.macromol.8b00238.

Lim, Z. W., Ping, Y., & Miserez, A. (2018). Glucose-responsive peptide coacervates with high encapsulation efficiency for controlled release of insulin. *Bioconjugate Chemistry*, *29*(7), 2176–2180. https://doi.org/10.1021/acs.bioconjchem.8b00369.

Lindhoud, S., & Claessens, M. M. A. E. (2016). Accumulation of small protein molecules in a macroscopic complex coacervate. *Soft Matter*, *12*(2), 408–413. https://doi.org/10.1039/C5SM02386F.

Lindhoud, S., de Vries, R., Schweins, R., Cohen Stuart, M. A., & Norde, W. (2009). Salt-induced release of lipase from polyelectrolyte complex micelles. *Soft Matter*, *5*(1), 242–250. https://doi.org/10.1039/B811640G.

Lindhoud, S., Norde, W., & Cohen Stuart, M. A. (2009). Reversibility and relaxation behavior of polyelectrolyte complex micelle formation. *The Journal of Physical Chemistry B*, *113*(16), 5431–5439. https://doi.org/10.1021/jp809489f.

Lindhoud, S., Voorhaar, L., de Vries, R., Schweins, R., Cohen Stuart, M. A., & Norde, W. (2009). Salt-induced disintegration of lysozyme-containing polyelectrolyte complex micelles. *Langmuir*, *25*(19), 11425–11430. https://doi.org/10.1021/la901591p.

Madinya, J. J., Chang, L.-W., Perry, S. L., & Sing, C. E. (2020). Sequence-dependent self-coacervation in high charge-density polyampholytes. *Molecular Systems Design and Engineering*, *5*, 632–644. https://doi.org/10.1039/C9ME00074G.

Martins, I. M., Barreiro, M. F., Coelho, M., & Rodrigues, A. E. (2014). Microencapsulation of essential oils with biodegradable polymeric carriers for cosmetic applications. *Chemical Engineering Journal*, *245*, 191–200. (C). https://doi.org/10.1016/j.cej.2014.02.024.

Nishida, K., Tamura, A., & Yui, N. (2018). pH-responsive coacervate droplets formed from acid-labile methylated polyrotaxanes as an injectable protein carrier. *Biomacromolecules*, *19*(6), 2238–2247. https://doi.org/10.1021/acs.biomac.8b00301.

Obermeyer, A. C., Mills, C. E., Dong, X.-H., Flores, R. J., & Olsen, B. D. (2016). Complex coacervation of supercharged proteins with polyelectrolytes. *Soft Matter*, *12*, 3570–3581. https://doi.org/10.1039/C6SM00002A.

Olson, B. J. S. C., & Markwell, J. (2007). *Assays for determination of protein concentration*. Hoboken, NJ: John Wiley & Sons, Inc., (pp. Unit3.4–3.4.29). Vol. Chapter 3.

Perry, S., Li, Y., Priftis, D., Leon, L., & Tirrell, M. (2014). The effect of salt on the complex coacervation of vinyl polyelectrolytes. *Polymers*, *6*(6), 1756–1772. https://doi.org/10.3390/polym6061756.

Priftis, D., Megley, K., Laugel, N., & Tirrell, M. (2013). Complex coacervation of poly(ethylene-imine)/polypeptide aqueous solutions: Thermodynamic and rheological characterization. *Journal of Colloid and Interface Science*, *398*, 39–50. https://doi.org/10.1016/j.jcis.2013.01.055.

Priftis, D., & Tirrell, M. (2012). Phase behaviour and complex coacervation of aqueous polypeptide solutions. *Soft Matter*, *8*(36), 9396–9405. https://doi.org/10.1039/C2SM25604E.

Schmitt, C., & Turgeon, S. L. (2011). Protein/polysaccharide complexes and coacervates in food systems. *Advances in Colloid and Interface Science*, *167*(1–2), 63–70. https://doi.org/10.1016/j.cis.2010.10.001.

Simonian, M. H. (2002). Spectrophotometric determination of protein concentration. *Current Protocols in Cell Biology*, *15*(1), A.3B.1–A.3B.7. https://doi.org/10.1002/0471143030.cba03bs15.

Stoscheck, C. M. (1990). Quantitation of protein. *Methods in Enzymology*, *182*, 50–68.

Thermo Scientific. (2010). *Protein A280*. Thermo Scientific, pp. 1–32.

Vehlow, D., Schmidt, R., Gebert, A., Siebert, M., Lips, K., & Müller, M. (2016). Polyelectrolyte complex based interfacial drug delivery system with controlled loading and improved release performance for bone therapeutics. *Nanomaterials*, *6*(3), 53. 21. https://doi.org/10.3390/nano6030053.

Water, J. J., Schack, M. M., Velazquez-Campoy, A., Maltesen, M. J., van de Weert, M., & Jorgensen, L. (2014). Complex coacervates of hyaluronic acid and lysozyme: Effect on protein structure and physical stability. *European Journal of Pharmaceutics and Biopharmaceutics*, *88*(2), 325–331. https://doi.org/10.1016/j.ejpb.2014.09.001.

Xu, Y., Liu, M., Faisal, M., Si, Y., & Guo, Y. (2017). Selective protein complexation and coacervation by polyelectrolytes. *Advances in Colloid and Interface Science*, *239*, 158–167. https://doi.org/10.1016/j.cis.2016.06.004.

Xu, Y., Mazzawi, M., Chen, K., Sun, L., & Dubin, P. L. (2011). Protein purification by polyelectrolyte coacervation: Influence of protein charge anisotropy on selectivity. *Biomacromolecules*, *12*(5), 1512–1522. https://doi.org/10.1021/bm101465y.

Yan, Y., Kizilay, E., Seeman, D., Flanagan, S., Dubin, P. L., Bovetto, L., et al. (2013). Heteroprotein complex coacervation: Bovine β-lactoglobulin and lactoferrin. *Langmuir*, *29*(50), 15614–15623. https://doi.org/10.1021/la4027464.

Yeo, Y., Bellas, E., Firestone, W., Langer, R., & Kohane, D. S. (2005). Complex coacervates for thermally sensitive controlled release of flavor compounds. *Journal of Agricultural and Food Chemistry*, *53*(19), 7518–7525. https://doi.org/10.1021/jf0507947.